

Published in *Chemical Communications International Journal for Chemistry* 75(17): 35–38, 2015
which should be cited to refer to this work.

Artificial Lysosomal Platform to Study Nanoparticle Long-term Stability

Ana Milosevic^{ac}, Joël Bourquin^a, David Burnand^{af}, Philipp Lemal^a, Federica Crippa^a, Christophe A. Monnier^{ae}, Laura Rodriguez-Lorenzo^{ad}, Alke Petri-Fink^{ab}, and Barbara Rothen-Rutishauser^{*a}

Abstract: Nanoparticles (NPs) possess unique properties useful for designing specific functionalities for biomedical applications. A prerequisite of a safe-by-design and effective use in any biomedical application is to study NP–cell interactions to gain a better understanding of cellular consequences upon exposure. Cellular uptake of NPs results mainly in the localization of NPs in the complex environment of lysosomes, a compartment which can be mimicked by artificial lysosomal fluid. In this work we showed the applicability of lysosomal fluid as a platform for a fast assessment of gold, iron oxide and silica NP stability over 24 h in a relevant biological fluid, by using multiple analytical methods.

Keywords: Artificial lysosomal fluids · Cell uptake · Engineered nanoparticles · Lysosomes · Stability

methods usually focus on cellular uptake mechanisms and induction of responses, but neglect the investigation of the potential physico-chemical changes of NPs inside cells including colloidal stability and possible dissolution.

Endocytosis of NPs results in the localization of these particles initially in early and late endosomes, which eventually fuse with lysosomes.^[2] Lysosomes are complex digestive organelles that have a low pH (~4.5), a salt-rich environment, and are filled with hydrolytic enzymes. Considering these factors, it can be expected that such a complex environment can alter the stability and integrity of NPs.^[3]

In previous years, different buffered solutions were used to simulate the lysosomal environment. For example, phosphate buffered saline (PBS) was supplemented with proteolytic enzymes,^[4] pH 4.5 adjusted PBS supplemented with enzymes^[5] and phosphate,^[6] acetate^[7] or citrate buffers at pH 4.5,^[7,8] were used. Although the previously named fluids replicate certain aspects of the lysosomal environment (pH, complex salt environment and presence of enzymes), they do not adequately mimic it. Artificial lysosomal fluid (ALF) has emerged as a fluid that simulates the environment of lysosomes in terms of pH, ionic strength, multiple components (presence of various inorganic and organic salts) and even the crowdedness of the given environment (increase of viscosity). ALF contains 13 inorganic and organic components and has been previously used to evaluate the bioavailability of metals,^[9] silica NP degradation^[10] and functionalized gold NP aggregation.^[6] ALF has previously been proven to be a more relevant environment for the prediction of intracellular NP behaviour compared to a simple buffer at pH 4.5.^[6]

Here we assessed the stability of biomedically relevant NPs, *i.e.* gold (AuNPs), superparamagnetic iron oxide (SPIONs) and silica (SiO₂) in ALF by UV-Vis spectroscopy and cryo electron microscopy, and compared our findings to their behaviour in cells, *i.e.* uptake and intracellular localization during exposure experiments by confocal and dark field imaging.

Introduction

The great potential of engineered nanoparticles (NPs) for biomedical applications requires a thorough and basic understanding on how these different particles interact with physiological fluids, and in particular with single cells.^[1] There is a need for simple and inexpensive methods for NP screening, in terms of their intracellular behaviour and stability, at early NP development stages. The most commonly reported *in vitro*

*Correspondence: Prof. B. Rothen-Rutishauser^a

E-mail: barbara.rothen@unifr.ch

^aAdolphe Merkle Institute, Faculty of Science and Medicine, University of Fribourg, Chemin des Verdiers 4, CH-1700 Fribourg

^bDepartment of Chemistry, University of Fribourg, Chemin du Musée 9, CH-1700 Fribourg

^cSwiss Federal Laboratories for Materials Science and Technology (Empa), Lerchenfeldstrasse 5, CH-9014 St. Gallen

^dINL – International Iberian Nanotechnology Laboratory, Avenida Mestre José Veiga 4715-330 Braga, Portugal

^eWaite Research Lab, Molecular, Cellular and Developmental Biology, University of California, Santa Barbara, USA

^fFederal Department of Economic Affairs, Education, and Research, EAER, Laboratory of ‘Proteins & Metabolites’, Agroscope, Schwarzenburgstr. 161, CH-3003 Bern

Results and Interpretation

ALF was prepared as previously reported.^[9] Briefly, sodium chloride (3.210 g), sodium hydroxide (6.000 g), citric acid (20.800 g), calcium chloride (0.097 g), sodium phosphate heptahydrate (0.179 g), sodium sulfate (0.039 g), magnesium chloride hexahydrate (0.106 g), glycerin (0.059 g), sodium citrate dihydrate (0.077 g), sodium tartrate dihydrate (0.090 g), sodium lactate (0.085 g), sodium pyruvate (0.086 g), formaldehyde (1.000 mL, added fresh before use) were dissolved in 200 mL of MiliQ water in order to obtain a 5× stock solution, that was later diluted with MiliQ water and NPs during incubation.

Hetero-functionalized amine-functionalized polyvinylalcohol (PVA) coated AuNPs (NH₂PVA AuNPs) with a fluorescent dye sandwiched between two polymer layers, silica NPs with fluorescent dye incorporated in the core and PVA-coated SPIONs with a fluorescent dye present on the surface, were prepared as described^[11–13] and the characterization results of the particles are shown in Table 1.

Table 1. NP size measurements, where the diameter of the core and the hydrodynamic diameter were obtained via TEM and DLS respectively.

Nanoparticle type	Core diameter (nm)	Hydrodynamic diameter (nm)
NH ₂ PVA AuNPs	17±4	68±18
SiO ₂ NPs	71±8	96±42
PVA SPIONs	22±2	70±30

NP aggregation and/or dissolution in ALF was assessed after 24 h incubation at 37 °C *via* cryo electron microscopy (CryoEM) (Fig. 1). The CryoEM served as a powerful tool to observe the stability of NPs in their native condition as it eliminates potential drying artefacts, which could be mistaken for aggregation.^[14] Another common technique for colloidal stability assessment is dynamic light scattering (DLS) which has advantage in the numbers of NPs analyzed in one measurement, but data analysis in complex fluids can be advanced. Special modes like depolarized DLS, which enables measurement in complex fluids, are in this case applicable only for AuNPs.^[15] Fig. 1A shows that throughout the incubation, NH₂PVA AuNPs remained stable in ALF. In the case of silica NPs, CryoEM micrographs indicate slight aggregation (Fig. 1B, white arrow). This can be explained by the lack of a surface-grafted polymer, such as PVA, which provides steric stabilization. In the case of the polymer-coated SPIONs, no aggregation was observed, however, only few NPs were detected after 24 h incubation in ALF (Fig. 1c). This observation could be an

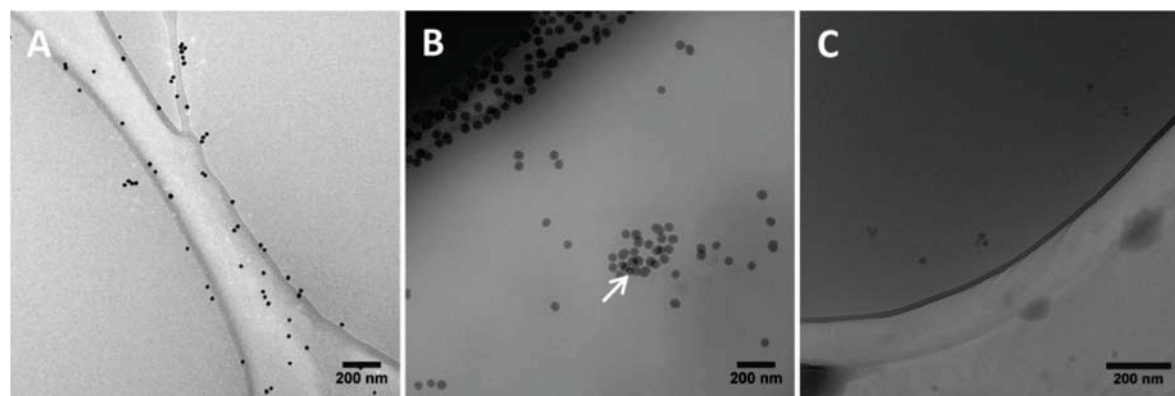


Fig. 1. Observation of NP stability by CryoEM. NPs, namely 0.05 mg/mL NH₂PVA AuNPs (A), 0.5 mg/mL silica NPs (B) and 0.5 mg/mL SPIONs (C) were incubated for 24 h at 37 °C in ALF prior to sample preparation and imaging under native conditions. The white arrow indicates the presence of silica NP aggregates

indication of NP dissolution, which was previously described for SPIONs upon 24 h incubation in an acidic solution, *i.e.* citric buffer pH 4.5.^[7,8] To further assess NP stability in ALF, all three NP types were incubated in ALF under the above-mentioned conditions, and consequently UV–Vis spectra were measured and images of the dispersion were taken at the beginning (0 h) and at the end of incubation (24 h) (Fig. 2). Fluorescent labelling is often used in biomedicine to allow NP intracellular tracking, however, fluorescence can be readily impaired by NP aggregation and dissolution.^[6,16] The fate of the fluorescent dye which was used to functionalize all NPs investigated here, was of particular interest in the case of silica NPs and SPIONs as the particles showed aggregation and potential dissolution in ALF, respectively.

Following the incubation of SPIONs in ALF, a significant loss of the SPIONs' characteristic colour was observed, while at the same time the colour originating from the fluorescent dye used for its functionalization (Rhodamine B) became more apparent (Fig. 2A, inserted image). These observations further indicate the dissolution of SPIONs, while for silica and NH₂PVA AuNPs no visual change was detectable (Fig. 2B and C, inserted images). Furthermore, the UV–Vis spectra of SPIONs revealed that the incubation in ALF resulted in a significant decrease in absorbance in the 200–300 nm and >400 nm range after 24 h (Fig. 2A, black solid and dashed line). Considering this and the images taken (Fig. 2A), one can further conclude that the SPIONs dissolve in the ALF. To determine if the fluorescent dye dissociates from the NPs due to particle dissolution, NPs incubated in ALF were centrifuged and their spectra were measured (Fig. 2A, red solid and dashed line). It was observed that the signal resulting from the fluorescent dye absorbance (500–600 nm) is more prominent for the NPs incubated in ALF (Fig. 2A spectra zoom in inset). The higher signal in the range below 500 nm is the result of the free polymer found in ALF following dissolution^[17] (Fig. 2A, red solid and dashed line). These findings indicate dissolution of SPIONs under intracellular conditions and are in agreement with CryoEM results. The potential dissolution of SPIONs in ALF was further confirmed by the presence of free iron ions which were only detected in the supernatant of SPIONs incubated in ALF and not PBS (data not shown). In the case of silica NPs, which previously only showed signs of aggregation in ALF, and not dissolution, the fluorescent dye remained incorporated in the NPs and no release was detected (Fig. 2B, spectra zoom in inset, red solid and dashed line). This finding is in agreement with a previous study by Dawson, where it was shown that silica NP integrity is not affected by ALF.^[10] UV–Vis spectroscopy of NH₂PVA AuNPs in ALF did not show a significant red shift in the UV–Vis spectra, nor could a change in colour be observed, indicating that the colloidal stability of the NPs was preserved (Fig. 2C and inserted image).^[5,6] Furthermore, the presence of

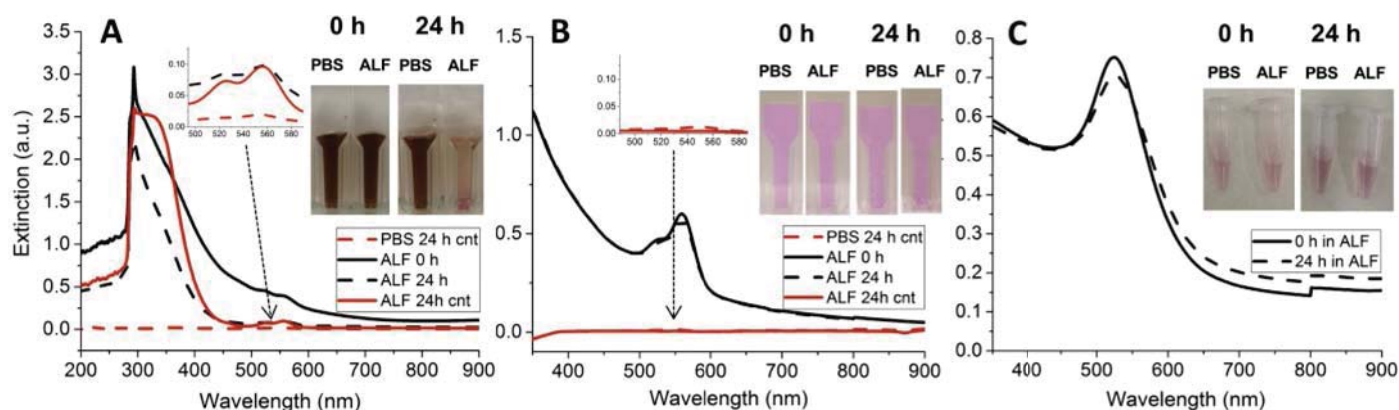


Fig. 2. Observation of NP stability by UV-Vis spectroscopy. NPs, namely SPIONs (A), silica NPs (B) and $\text{NH}_2\text{PVA AuNPs}$ (C) were incubated for 24 h at 37 °C in both PBS and ALF. UV-Vis spectra were measured and pictures were taken at the beginning of incubation (0 h) and at the end (24 h). Significant dye loading in the case of SPIONs and silica NPs allowed for assessment of dye detachment from the NP by direct measurement of supernatant after NP centrifugation (24 h cnt). Inset zoomed in spectra shows wavelength range where fluorescent dye is absorbing (500–580 nm).

free PVA polymer and consequently the dye could not be detected *via* colorimetric assay (data not shown).

In order to assess the applicability of ALF to mimic the lysosomal environment, we also assessed the fate of NPs in the cells by fluorescent microscopy. Such assessments have to be done with fluorescent NPs. However, the lysosomal environments can induce a loss or change in the NP fluorescent properties. In a previously published study, the quenching of fluorescent dyes caused by the close proximity to AuNP core for carboxylated PVA-coated particles, was observed both in ALF and in cells.^[6] To compare the findings with ALF, NPs were exposed to J774A.1 cells for 24 h and the particle localization was investigated by laser scanning microscopy (LSM) and for SPIONs also fluorescence-coupled dark field microscopy (FL-DF). The selected mouse macrophages (J774A.1) are often used to assess NP endocytosis pathways^[18] and cell responses,^[19] and are expected to provide representative results for other cell types, due to the universal role of lysosomes.^[20]

In the case of the $\text{NH}_2\text{PVA AuNPs}$ used in this study, an impairment of their fluorescent properties after cellular uptake was not observed and an intense particle staining was still observed after 24 h (Fig. 3A), which correlated well with the previous findings that ALF environment does not affect the stability of AuNPs. Even though silica NPs showed aggregation in CryoEM images, UV-Vis did not reveal any loss of the fluorescent dye. This comes as no surprise, since the fluorescent dye is embedded within the nanoparticles' core and, it was previously shown that after 24 h incubation, ALF does not degrade silica NPs.^[10] In correlation

with those findings intracellular silica NPs remained fluorescent (Fig. 3C)

The intracellular fate of SPIONs showed some striking results, where the fluorescent signal of SPIONs, incubated with cells, suggested that NPs were localized in the cell nucleus (Fig. 3B). The red signal originating from functionalized SPIONs was also observed in the cytoplasm, but to a lesser degree than the signal localized in the nucleus, completely overlapping the signal originating from the nucleus stain DAPI (blue), resulting in the fuchsia colour.

To assess whether the localization of the fluorescent signal corresponds to the presence of the SPIONs themselves, FL-DF imaging was used. Once again, the signal originating from the fluorescent dye (red) overlapped with the nucleus stain DAPI (blue), resulting in a fuchsia signal, while the signal originating from the SPIONs, caused by light scattering, did not overlap with signals of either the Rhodamine or DAPI. Quite contrary, DF-HSI could not detect any signal originating from the iron in the cell nucleus. The separation of fluorescent dye and the core in the cells confirms what we observed in ALF. It can be hypothesized that the diffusion of NP-unassociated dye into the nucleus is the consequence of SPION dissolution.^[7,8] A similar intracellular dissolution of iron oxide nanocubes was observed by Lartigue *et al.*,^[21] by using aberration corrected high resolution transmission electron microscopy.

From the previous data, the ALF platform proved to be a reliable method for initial intracellular assessment, and can give insight in both potential aggregation as it was in the case of silica

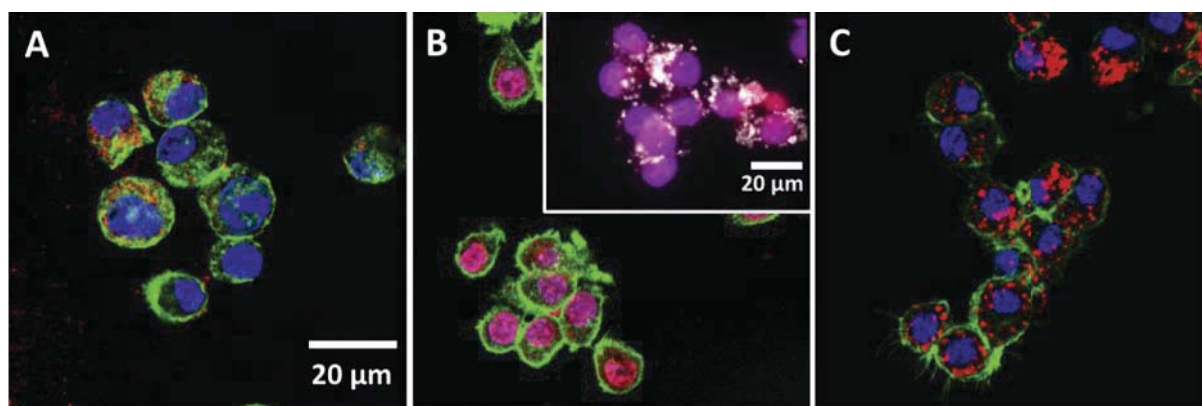


Fig. 3. Intracellular localization of NPs. Particles were incubated for 24 h at 37 °C in J774 A.1 cells. Cells were stained with a nucleus stain DAPI (blue), a F-actin stain phalloidin Alexa 488 (green) and particles were functionalized with (A) ATTO590 dye in the case of $\text{NH}_2\text{PVA AuNPs}$, (B) Rhodamine dye (red) in the case of SPIONs and (C) Rhodamine dye (red) in the case of silica NPs. In the case of SPIONs, LSM was complemented by FL-DF (B: white box inset) and cells were stained with a nucleus stain DAPI (blue), and SPIONs were labelled with a Rhodamine stain (red). The signal resulting from the light scattering, caused by the SPIONs' core is shown in silver/white.

NPs, and dissolution which was observed for SPIONs in the complex environment of lysosomes. Moreover, obtained data correlated well with the behaviour of NPs in lysosomes and, depending on the NP type, clear differences in the behaviour could be observed after 24 h, which can be used as initial assessment on the potential of NPs intended for biomedical application. Furthermore, to mimic the fate of NPs *in vivo* over a longer time period, the assay can be used to investigate the stability of NPs over several weeks in ALF.

Acknowledgment

AM, APF and BRR would like to acknowledge the National Center of Competence in Research for Bio-Inspired Materials, JB and BRR the Swiss National Science Foundation (310030_159847/1), and all authors acknowledge the Adolphe Merkle Foundation for financial support.

- [1] A. E. Nel, L. Mädler, D. Velegol, T. Xia, E. M. V. Hoek, P. Somasundaran, F. Klaessig, V. Castranova, M. Thompson, *Nat. Mater.* **2009**, *8*, 543.
- [2] T. G. Iversen, T. Skotland, K. Sandvig, *Nano Today* **2011**, *6*, 176.
- [3] T. L. Moore, L. Rodriguez-Lorenzo, V. Hirsch, S. Balog, D. Urban, C. Jud, B. Rothen-Rutishauser, M. Lattuada, A. Petri-Fink, *Chem. Soc. Rev.* **2015**, *44*, 6287.
- [4] W. G. Kreyling, A. M. Abdelmonem, Z. Ali, F. Alves, M. Geiser, N. Haberl, R. Hartmann, S. Hirn, D. J. de Aberasturi, K. Kantner, G. Khadem-Saba, J. M. Montenegro, J. Rejman, T. Rojo, I. R. de Larramendi, R. Ufartes, A. Wenk, W. J. Parak, *Nat. Nanotechnol.* **2015**, *10*, 619.
- [5] M. Chanana, P. Rivera-gil, M. A. Correa-Duarte, L. M. Liz-Marzán, W. J. Parak, *Angew. Chem. Int. Ed.* **2013**, *52*, 4179.
- [6] A. M. Milosevic, L. Rodriguez-Lorenzo, S. Balog, C. A. Monnier, A. Petri-Fink, B. Rothen-Rutishauser, *Angew. Chem. Int. Ed.* **2017**, *56*, 13382.
- [7] T. Skotland, P. C. Sontum, I. Oulie, *J. Pharm. Biomed. Anal.* **2002**, *28*, 323.
- [8] A. S. Arbab, L. B. Wilson, P. Ashari, E. K. Jordan, B. K. Lewis, J. A. Frank, *NMR Biomed.* **2005**, *18*, 383.
- [9] W. Stopford, J. Turner, D. Cappellini, T. Brock, *J. Environ. Monit.* **2003**, *5*, 675.
- [10] F. Meder, S. S. Thomas, L. W. Fitzpatrick, A. Alahmari, S. Wang, J. G. Beirne, G. Vaz, G. Redmond, K. A. Dawson, *ACS Nano* **2016**, *10*, 4660, doi: 10.1021/acsnano.6b01001.
- [11] L. Rodriguez-Lorenzo, K. Fytianos, F. Blank, C. Von Garnier, B. Rothen-Rutishauser, A. Petri-Fink, *Small* **2014**, *10*, 1341.
- [12] D. Burnand, C. A. Monnier, A. Redjem, M. Schaefer, B. Rothen-Rutishauser, A. Kilbinger, A. Petri-Fink, *J. Magn. Magn. Mater.* **2015**, *380*, 157.
- [13] D. R. Larson, H. Ow, H. D. Vishwasrao, A. A. Heikal, U. Wiesner, W. W. Webb, *Chem. Mater.* **2008**, *20*, 2677.
- [14] C. A. Monnier, D. C. Thévenaz, S. Balog, G. L. Fiore, D. Vanhecke, B. Rothen-Rutishauser, A. Petri-Fink, *AIMS Biophys.* **2015**, *2*, 245.
- [15] S. Balog, L. Rodriguez-Lorenzo, C. A. Monnier, M. Obiols-Rabasa, B. Rothen-Rutishauser, P. Schurtenberger, A. Petri-Fink, *Nanoscale* **2015**, *7*, 5991.
- [16] E. Muro, A. Fragola, T. Pons, N. Lequeux, A. Ioannou, P. Skourides, B. Dubertret, *Small* **2012**, *8*, 1029.
- [17] H. C. Haas, H. Husek, L. D. Taylor, *J. Polym. Sci. Part A Gen. Pap.* **1963**, *1*, 1215.
- [18] D. A. Kuhn, D. Vanhecke, B. Michen, F. Blank, P. Gehr, A. Petri-Fink, B. Rothen-Rutishauser, *Beilstein J. Nanotechnol.* **2014**, *5*, 1625.
- [19] C. F. Jones, D. W. Grainger, *Adv. Drug Deliv. Rev.* **2009**, *61*, 438.
- [20] H. Appelqvist, P. Wäster, K. Kågedal, K. Öllinger, *J. Mol. Cell Biol.* **2013**, *5*, 214.
- [21] L. Lartigue, D. Alloyeau, J. Kolosnjaj-Tabi, Y. Javed, P. Guardia, A. Riedinger, C. Péchoux, T. Pellegrino, C. Wilhelm, F. Gazeau, *ACS Nano* **2013**, *7*, 3939.